

# Elucidation of the structure of supramolecular polymorphs in peptide nanofibres using Raman spectroscopy

Sian Sloan-Dennison<sup>1</sup>  | Ayala Lampel<sup>2,3,4</sup> | Eileen Raßlenberg<sup>5</sup> |  
 Rein V. Ulijn<sup>6,7,8</sup> | Ewen Smith<sup>1</sup> | Karen Faulds<sup>1</sup> | Duncan Graham<sup>1</sup>

<sup>1</sup>Centre for Molecular Nanometrology, WestCHEM, Department of Pure and Applied Chemistry, Technology and Innovation, 99 George Street, Glasgow, G1 1RD, Scotland

<sup>2</sup>The Shmunis School of Biomedicine and Cancer Research, George S. Wise Faculty of Life Sciences, Tel Aviv University, Tel Aviv, 69978, Israel

<sup>3</sup>Sagol Center for Regenerative Biotechnology, Tel Aviv University, Tel Aviv, 69978, Israel

<sup>4</sup>The Center for Nanoscience and Nanotechnology, Tel Aviv University, Tel Aviv, 69978, Israel

<sup>5</sup>Organisch-Chemisches Institut, University of Muenster, Corrensstraße 40, Muenster, 48149, Germany

<sup>6</sup>Advanced Science Research Center (ASRC) at the Graduate Center, City University of New York (CUNY), New York, New York, USA

<sup>7</sup>Department of Chemistry, Hunter College, City University of New York, 695 Park Avenue, New York, New York, 10065, USA

<sup>8</sup>Ph.D programs in Biochemistry and Chemistry, The Graduate Center of the City, University of New York, New York, New York, 10016, USA

## Correspondence

Duncan Graham, Centre for Molecular Nanometrology, WestCHEM, Department of Pure and Applied Chemistry, Technology and Innovation, 99 George Street, Glasgow, G1 1RD, Scotland.  
 Email: duncan.graham@strath.ac.uk

## Funding information

U.S. Air Force Office of Scientific Research, Grant/Award Number: FA9550-19-1-0111; University of Strathclyde

## Abstract

Peptide fibre formation via molecular self-assembly is a key step in a range of cellular processes and increasingly considered as an approach to produce supramolecular biomaterials. We previously demonstrated the self-assembly of the tripeptide lysine-dityrosine (KYY) as a substrate for the formation of proton-conducting melanin-like materials. Point based Raman scattering is one of several techniques which were used to characterise the secondary structure of the KYY nanofibre but as is often the case with this type of fibre, the spectra are rather complex and in addition there were variations in intensity between samples making interpretation difficult. Using Raman mapping we show that, as a drop of KYY in solution dries, it self-assembles into two different fibre forms and the simpler spectra obtained for each are easier to interpret. The tyrosine amide marker bands, 852 and 828 cm<sup>-1</sup>, are present in both forms with similar intensities indicating the formation of a similar secondary structure in both forms with some stacking of the tyrosine rings. However, the tyrosine marker bands at 1614 and 1661 cm<sup>-1</sup> vary considerably in intensity between the two forms. It is concluded that both forms consist of stacked polypeptide units joined by hydrogen bonds to form structures similar to  $\beta$ -sheet structures in longer peptides. There are other clear differences such the large intensity difference in the lysine side chain band at 1330 cm<sup>-1</sup> and the relative intensities of the bands at 982 and 1034 cm<sup>-1</sup>. These differences are attributed

to changes in the conformation of tyrosine side chains causing different electron withdrawing effects on the ring.

#### KEY WORDS

peptides, Raman, self-assembly

## 1 | INTRODUCTION

Short peptide chains can self-assemble to form biomaterials with tuneable structures and properties.<sup>[1–3]</sup> During the self-assembly process, the peptides ability to adopt distinct secondary structures produces a wide range of well-defined nanostructures such as nanofibres, nanoribbons, nanospheres and nanorods.<sup>[4,5]</sup> Common forms of these secondary structures include the  $\alpha$ -helix, a right-handed helix where the peptide bonds are located on the inside and the side chains extend outwards, and  $\beta$ -sheets which consist of  $\beta$ -strands that are connected laterally by hydrogen bonds to produce a very rigid structure.<sup>[6]</sup> The flexible left-handed polyproline II (pP-II) helix can also occur when repeating proline residues are present.<sup>[7]</sup> Random coil structures are also a possibility where the monomer units are connected by bonds of fixed length and uncorrelated directions.<sup>[8]</sup>

The structural form of the biomaterial can affect the biological activity. For example, when peptides of certain sequence and charge density form an  $\alpha$ -helix, their bactericidal activity and cytotoxicity can increase. This is due to the  $\alpha$ -helix's amphipathic nature that segregates basic and hydrophobic residues into polar and non-polar faces.<sup>[9]</sup> Intermolecular interactions between the hydrogen bonds at the edges of  $\beta$ -sheets are involved in protein quaternary structure, protein–protein and peptide–protein interactions.<sup>[10]</sup> A negative consequence of this occurs when amyloid peptides convert into  $\beta$ -sheet rich structures which possess a neurotoxic activity and form insoluble deposits that accumulate in the brain, a key pathological event in Alzheimer's disease.<sup>[11]</sup> The design of much shorter peptides that can self-assemble into these secondary structures provides important model systems to help understand key biological activities. It is therefore important to understanding the forces that contribute to the stability of the interactions involved in the secondary structure.

Secondary structures have been characterised by many techniques such as circular dichroism (CD),<sup>[12]</sup> x-ray diffraction (XRD)<sup>[13]</sup> and nuclear magnetic resonance (NMR).<sup>[14]</sup> While each technique has a number of advantages, drawbacks include the inability of CD to determine secondary structure content for proteins with a mixed  $\alpha$ - and  $\beta$ -element in their structure, the

static picture provided by XRD and the limited amount of dynamic information obtained from NMR. Raman spectroscopy is relatively fast, non-invasive, and can be used to probe *in situ*. It can be used to elucidate secondary structures as was demonstrated by Chi et al. who utilised UV-resonance Raman to determine the wavenumbers associated with pure  $\alpha$ -helix,  $\beta$ -sheet and unordered proteins by using the amide resonance Raman spectra of 13 proteins.<sup>[15]</sup> Lekprasert et al have obtained structural information on diphenylalanine (FF) supramolecular assemblies using polarized Raman microspectroscopy and determined that the wavenumbers of the amide I and amide III bands indicated that the FF molecules were interacting via hydrogen bonding with the N-H bond.<sup>[16]</sup>

Recently, Lampel et al. reported the self-assembly of six tripeptide sequence isomers composed of tyrosine, phenylalanine and aspartic acid (Y, F, D). These tripeptides were subsequently used as tuneable precursors for tyrosine oxidation to form polymeric pigments to investigate the promise of peptide building blocks for the formation of melanin-like materials.<sup>[17]</sup> Using TEM, XRD and Fourier-transform infrared spectroscopy (FTIR), they demonstrated that the 6 peptides had different preferential conformations in solution, which was dependent on the positioning of tyrosine within the sequence at the C-terminus, N-terminus or in the centre. Following self-assembly, the resulting structures underwent enzymatic oxidation to form polymeric pigments, giving rise to different products with variable activities, demonstrating control and tunability over the properties of the material. They furthered this work by designing a tripeptide, lysine-tyrosine-tyrosine (KYY) precursor that self-assembles into supramolecular nanofibres, that retained their fibrillar morphology and present melanin-like properties after enzymatic oxidation.<sup>[18]</sup> In order to fully characterise the self-assembled nanofibres before oxidation, averaged point-based Raman spectroscopy was included in the analysis. Overall, the results suggested the nanofibres were in a  $\beta$ -sheet confirmation, however the Raman data was complex and variations in intensity were noted. In this paper we report Raman mapping experiments performed on the self-assembled KYY nanofibres. By analysing the Raman maps with false colour heat intensity images and principal component analysis (PCA)

we demonstrate that two different forms of the KYY fibre are present, and we obtain information about their structure. Many point-based spectra of polypeptide fibres reported to date show complex spectra and this study suggests that care should be taken to ascertain whether or not this is due to mixtures of fibres with different supramolecular morphologies.

## 2 | EXPERIMENTAL

KYY fibres were produced by dissolving KYY powder in d.H<sub>2</sub>O (30 mM, 14 mg/ml) and then tuning the pH of the solution to 7.5 using 0.5 M NaOH. Raman spectra were acquired on a Renishaw InVia Raman microscope equipped with a 532 nm Nd:YAG laser and 785 nm diode laser with a power of 2.5 mW at sample, 1800 lines/mm grating and Leica 20X/NA 0.4 N PLAN EPI objective. The Raman spectrum of tyrosine, lysine and KYY powder was acquired by placing ~1 mg onto a clean calcium fluoride slide. Using a 20x objective, the laser was focused onto the powder and an average of three extended scans (3200–100 cm<sup>-1</sup>), with a 10-s acquisition time, were acquired using 532- or 785-nm laser excitation. Mapping samples were prepared by spotting 1 µl of the KYY nanofibre onto a clean calcium fluoride slide which was left to dry. Raman maps were obtained using a 20X objective with a centred scan at 1130 cm<sup>-1</sup>, a 1-s acquisition time and 5 × 5-µm step size. All spectra were baseline corrected using the baseline subtract function available on WiRE TM software. False colour images and PCA analysis were carried out using WiRE TM software.

## 3 | RESULTS AND DISCUSSION

The previously reported point-based Raman analysis of KYY nanofibres assigned the spectrum to a supramolecular system in a β-sheet confirmation.<sup>[18]</sup> However, a fuller elucidation of the nanofibre was achieved in this study by providing more detailed spectroscopic interpretation on the system using Raman mapping analysis. First, the Raman spectra of the tripeptide KYY powder, structure shown in Figure 1a, tyrosine and lysine were collected and are shown in Figure S1 (supporting information). The peaks in the KYY powder spectrum originating from tyrosine (giving them the Y terminology), which have previously been numbered by Hernandez et al, are 1616 (Y1), 1600 (Y2), 1210 (Y3), 1170 (Y4), 852 (Y5) and 828 (Y6) cm<sup>-1</sup>.<sup>[19]</sup> Fewer peaks in the KYY powder can be associated with lysine, but the large peak at 1444 cm<sup>-1</sup> is assigned to C-H bending and twisting displacements on the lysine side chain, possibly with some N-H displacement as well.<sup>[20]</sup> The peak at 1744 cm<sup>-1</sup> in the powder is due to retained solvent. Self-assembly into KYY nanofibres was initiated by dissolving the freeze-dried peptide powder in water at pH 7.5, shown in the white light image in Figure 1b. The equivalent of a single point 532 nm Raman spectrum was obtained by drying out a drop of the solution on a calcium fluoride slide and averaging the spectra obtained from several points on the slide. The normalised averaged Raman spectrum is compared to the KYY powder spectrum in Figure 1c. There are many differences in the spectrum upon fibre formation including significant changes in the weaker bands in the

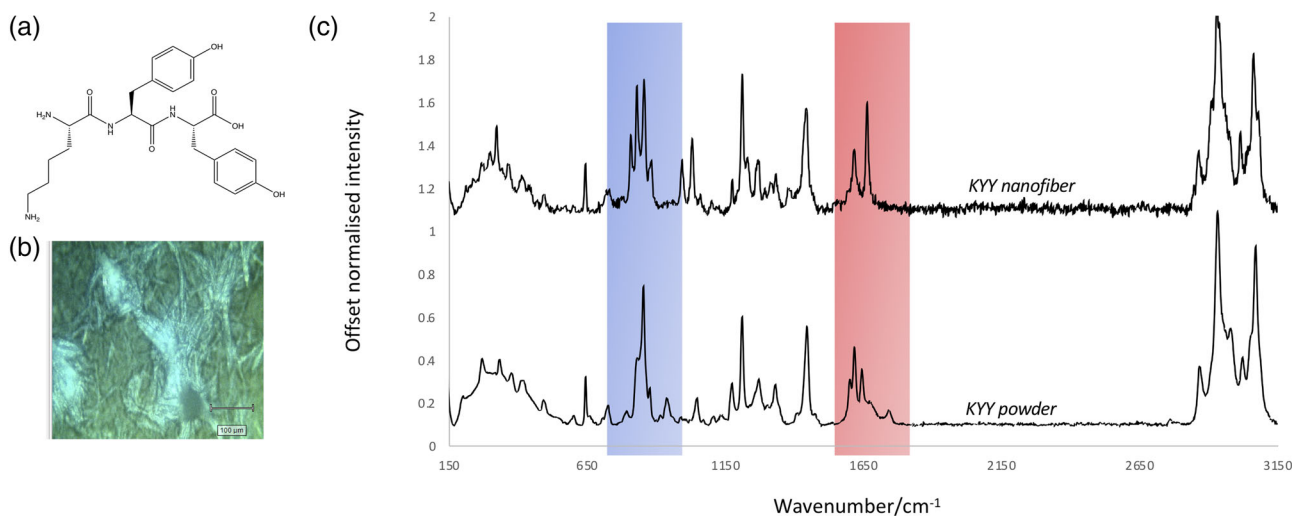


**FIGURE 1** (a) Structure of KYY tripeptide. (b) White light image of KYY fibres taken using 20X objective. (c) Normalised Raman spectra of KYY powder and KYY fibre. Wavenumber region highlighted in blue contain the Y5 and Y6 tyrosine bands and the region highlighted in red contains the Y1 and Y2 bands. Spectra were obtained using a 20X objective with an extended scan (3,200–100 cm<sup>-1</sup>), 10-s acquisition time and a 532-nm laser excitation [Colour figure can be viewed at [wileyonlinelibrary.com](http://wileyonlinelibrary.com)]

900–1050 cm<sup>-1</sup> region but the most diagnostic are the changes in the regions between 800 and 900 cm<sup>-1</sup>, highlighted in blue and 1,600–1750 cm<sup>-1</sup>, highlighted in red which contain the tyrosine amide marker bands Y5, Y6 and Y1, Y2. The other tyrosine amide marker bands are less affected.

Repeat measurements on different parts of the fibre, and single point spectra obtained with different excitation frequencies showed variation in relative peak intensities between the 1,614 and 1,616 cm<sup>-1</sup> peaks suggesting that the fibre may not be homogeneous. To explore this further, the KYY fibre coated slide was Raman mapped using 532-nm laser excitation. False colour heat intensity images were created by monitoring

the 1661-cm<sup>-1</sup> peak, Figure 2b and 1614 cm<sup>-1</sup>, Figure 2c. The images demonstrated the variation in peak intensity throughout the fibre and also the changing ratio of the two peaks. This is better represented when comparing the normalised Raman spectra from an area of the fibre where either the 1661 or 1614 cm<sup>-1</sup> was most intense and is shown in Figure 2i. The spectra have been assigned as being representative of form 1, which has an intense 1661-cm<sup>-1</sup> peak and form 2, which has an intense 1614-cm<sup>-1</sup> peak. The small number of peaks and large intensity change in both peaks in the 1600 to 1700 cm<sup>-1</sup> region suggests that there are only two forms present. Repeat mapping experiments and analysis are shown in Figure 2e–g.

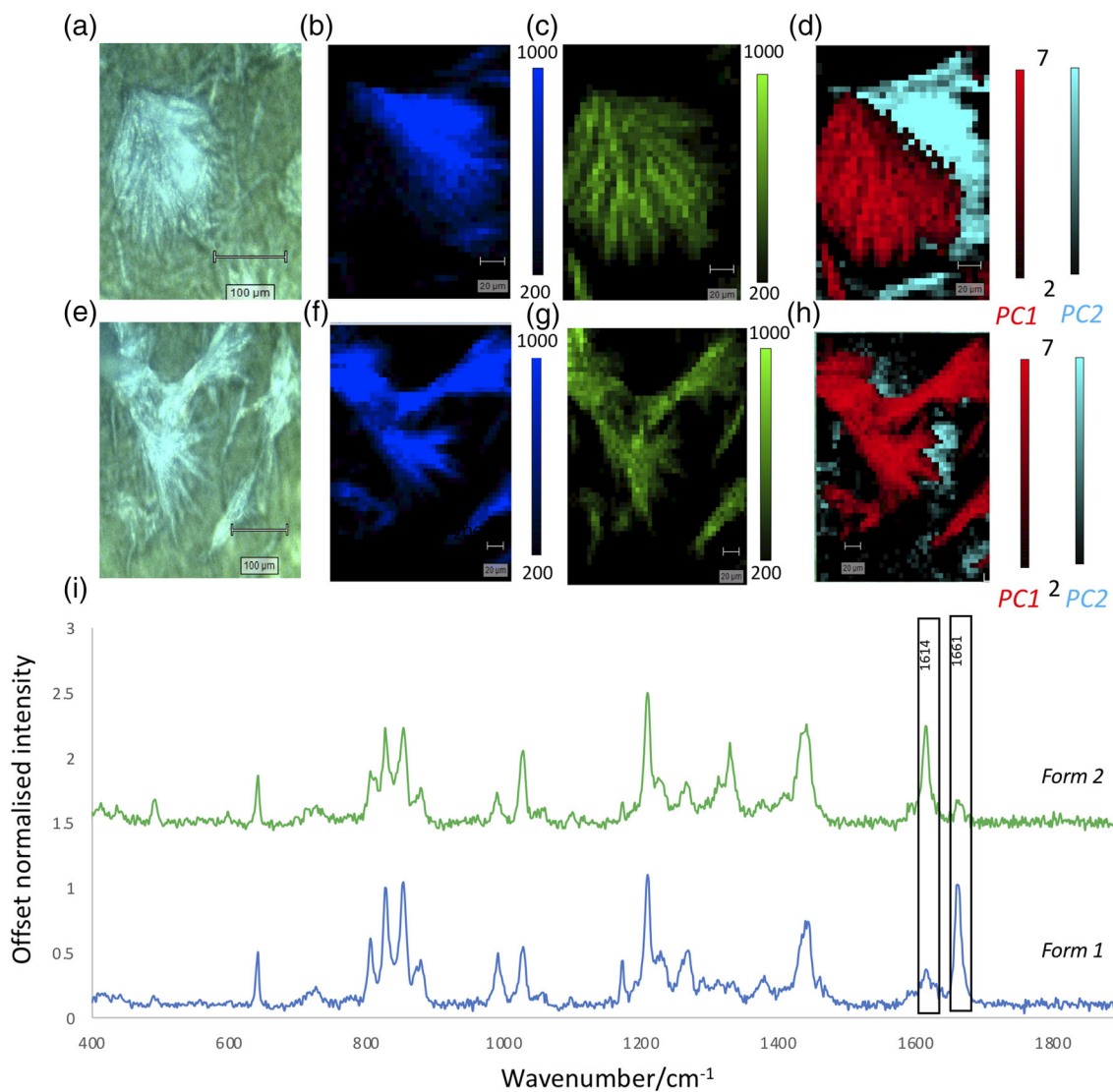


**FIGURE 2** (a) White light image of KYY fibre area mapped. (b) False colour image of map created using 1661 cm<sup>-1</sup> peak. (c) False colour image of map created using 1614 cm<sup>-1</sup> peak. (d) False colour image created from principal component analysis (PCA) analysis using the loading plot of principal component 1 (red) and the loadings plot of principle component 2 (cyan). (e-h) show repeat analysis. (i) Normalised spectrum of form 1 (blue) and form 2 (blue). KYY fibres mapped with a centred scan at 1130 cm<sup>-1</sup>, a 1-s acquisition time and 5 × 5 μm step size, 532-nm laser excitation and 2.5-mW laser power [Colour figure can be viewed at [wileyonlinelibrary.com](http://wileyonlinelibrary.com)]

To investigate this further, a more in-depth representation of the differences between the two forms was obtained and a false colour image created using principal component analysis (PCA) is shown in Figures 2d and 2h. It indicated the areas which are most representative of component 1 (red) and component 2 (cyan) and the loading plots associated with each component are shown in Figures S2 and S3 (supporting information). The PCA false colour image indicates that PC1 occurs where the  $1614\text{ cm}^{-1}$  peak was intense (form 2) and PC2 where the  $1616\text{-cm}^{-1}$  peak was intense (form 1). Additional information was obtained from analysing the loading plots. Positively correlated peaks on the loading plot of component 1 included the already known  $1614\text{ cm}^{-1}$  peak but also identified  $1330$ ,  $1436$  and  $1034\text{ cm}^{-1}$  as prominent peaks of form 2. There are far fewer positively correlated peaks in the loading plot of component 2 as the  $1661\text{ cm}^{-1}$  peak was so dominant; however, there were other positively correlated peaks at  $992$ ,  $1380$  and  $1458\text{ cm}^{-1}$  which are present in form 1. These peaks were then used to assign possible structures of each form.

Although Raman scattering alone cannot provide complete structural information on such a complex system, previous work on tyrosine marker bands Y1, Y2, Y5 and Y6 enables an indication of the nature of the fibres obtained. Since one likely use of Raman spectra is in metabolic studies, where Raman scattering enables *in situ* detection in tissue and fluid, any information which can be obtained is of value. Therefore, we considered the spectra in these regions in more detail.

Typical powder tyrosine Raman spectra gives a strong band at  $852\text{ cm}^{-1}$  (Y5) due to an in-plane mode of the aromatic ring and a weaker out of plane mode (Y6) at about  $830\text{ cm}^{-1}$ , although this was found to be reversed in tyrosine crystals. Hernandez et al have investigated this region both practically and theoretically for tyrosine including some tripeptide measurements.<sup>[15]</sup> The ratio of Y5/Y6 is very sensitive to the environment since Y6 is an out of plane mode, the intensity of which would be forbidden in an ideal geometry. Its magnitude depends on the influence of the substituents on the aromatic ring which varies depending on the environment. For KYY, the bonding of one substituent into the polypeptide chain will influence the spectra as does the OH group which for the middle tyrosine, from theoretical calculations, is likely to be bonded to the peptide chain. The pattern of four peaks in the KYY nanofibre at  $804$ ,  $832$ ,  $852$  and  $877\text{ cm}^{-1}$  has some similarities to that found in some clusters of tyrosine at neutral pH which have been shown to be strongly influenced by ring stacking.<sup>[15]</sup> Thus, the spectra indicate that both forms of KYY have some ring stacking which is intermediate between the fully stacked arrangement in tyrosine crystals and no stacking. Since

both forms of KYY show similar, although not identical spectra, spectral intensities in this region are quite sensitive to the environment and consequently, the packing in both structures is probably quite similar. Thus, a picture emerges of tripeptide units with some stacking of the tyrosine rings and hydrogen bonding interactions. Given the geometric constraints caused by stacking, it is likely that the units are connected by the ends of the tripeptide through hydrogen bonding. It should be noted that the two forms were separated so successfully using PCA due to the nanofibres drying on the slide from one side to the other, and it can be proposed that they have different solubilities, therefore any water molecules incorporated in the structure may also interact.

The band at  $1661\text{ cm}^{-1}$ , which is intense in form 1, has been assigned in most studies as the amide I band of proteins and peptides in a true, insoluble  $\beta$  sheet conformation.<sup>[15,21]</sup> Other evidence of this is the  $1,229\text{ cm}^{-1}$  band which is commonly assigned to the amide III in  $\beta$  sheets<sup>[15]</sup> and PCA indicated the peak at  $1380\text{ cm}^{-1}$ , regularly assigned to the  $C_{\alpha}\text{-H}$  bending band of a  $\beta$  sheet, was also unique to this form. However, describing this structure as a true  $\beta$  sheet is inappropriate as longer peptide chains are generally needed for  $\beta$  sheet assembly. It is proposed that the anti-backbone torsion angles ( $\Phi_2, \Psi_2$ ) of KYY adopt values close to that of a  $\beta$  sheet.<sup>[22]</sup> Thus, a picture emerges of tripeptides ordered in a structure analogous to the  $\beta$  sheet arrangement found in longer peptide chains but with tripeptide units joined by hydrogen bonding. Figure 3a gives an illustrative interpretation of the structure of form 1 due to the ring stacking interactions from phenol rings of the tyrosine side chain and the hydrogen bonding between parallel tripeptides.

Hernández et al. investigated the structure of four tripeptides carefully considering hydration effects and demonstrated that the presence of five water molecules around the backbone can considerably change the secondary structure.<sup>[22]</sup> In their analysis the population of pP-II and helical conformers dominated in the presence of water molecules due to their stability. Therefore, the difference observed in form 2 was attributed to the presence of water molecules interacting with the peptide backbone of this soluble form of the KYY fibre. The structure of form 2 has been assigned from the Raman spectrum. The band at  $1614\text{ cm}^{-1}$ , present in form 2, has been used in some papers to indicate either a disordered or an  $\alpha$ -helix type structure in longer peptides. However, Profit et al. investigated  $\pi\text{-}\pi$  stacking in the self-assembly of peptide analogs using phenylalanine and reported that the intense  $1,670\text{ cm}^{-1}$  peak formed on self-assembly indicated  $\beta$ -sheet formation and the  $1,614\text{ cm}^{-1}$  was largely due to a quadrant stretching mode of the tyrosine ring, indicative of a  $\pi\text{-}\pi$  stacking contribution associated

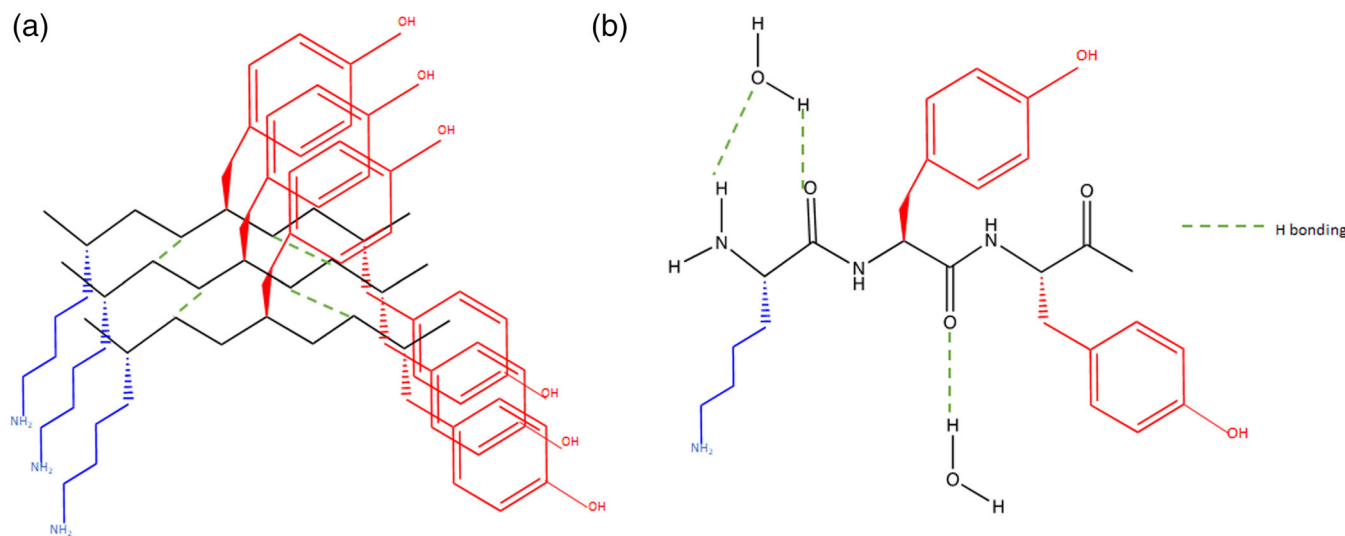


**FIGURE 3** (a) Form 1, insoluble beta sheet with tyrosine ring stacking and hydrogen bonding between parallel strands. (b) Form 2, soluble beta sheet with water molecules hydrogen bonding to peptide backbone leading to more distorted long range geometry [Colour figure can be viewed at [wileyonlinelibrary.com](http://wileyonlinelibrary.com)]

with  $\beta$ -sheet formation.<sup>[23]</sup> We conclude that based on the analysis and differences observed in the Y1 and Y2 region and the similarities of the Y5 and Y6 region, that this second form of the fibre has a very similar tripeptide arrangement to the first form with changes in stacking modifications between the tyrosine rings (aromatic-aromatic interactions) or between phenol rings and Lys side chains. It is proposed that the difference is due to water molecules hydrogen bonding to the peptide backbone. Therefore, form 2 is the more soluble form of the fibre. This is illustrated in Figure 3b which shows the potential H-bonding sites of the water molecules.

There are other clear differences between the spectra of the two bands which act as markers but their assignment is difficult. The band at  $1330\text{ cm}^{-1}$ , assigned in previous papers mainly to C-H displacements, is very weak in form 1. This has been observed before in a  $\beta$ -sheet arrangement for poly-L-lysine,<sup>[24]</sup> but in the form which gives the form 2, the intensity compared to the lysine band is similar to that in many lysine spectra including  $\alpha$ -helix and other structures. This may suggest that this form has a more distorted long range geometry in the fibre but not an  $\alpha$ -helix since a separate band should appear in the  $1,600$  to  $1,700\text{-cm}^{-1}$  region indicating this structural motif.<sup>[25]</sup>

Finally, medium strength bands appear at  $982$  and  $1034\text{ cm}^{-1}$ , which are correlated by PCA to belong to one or other of the forms. They make effective markers of fibre formation but are difficult to assign with any certainty. There are a number of bands in this region in many lysine spectra assigned previously to be due to C-C displacements on the side chain and the spectra from the

fibres are simple by comparison with many spectra. This may suggest a more defined arrangement of the lysine side chains which is likely in any case since the amine group will be positively charged and therefore probably ordered in the lattice.

#### 4 | CONCLUSION

This work clearly shows that when KYY fibres are formed by self-assembly followed by precipitation from aqueous solution and dried, two forms of fibre with different solubilities are obtained which together explain the single point Raman spectrum obtained previously. The results show that two commonly used marker regions, often used to understand peptides, behave very differently. The  $800$  to  $860\text{ cm}^{-1}$  region shows little change suggesting similar structures between the two forms whereas the  $1600$  to  $1700\text{ cm}^{-1}$  region shows large changes in intensity, but not wavenumber, between the two forms. We conclude that the lower wavenumber region is most influenced by packing and local structural variations whereas the  $1600$  to  $1700\text{ cm}^{-1}$  region is also influenced by the electron withdrawing potential of the side chains which will depend on hydrogen bonding and hydrophobicity. Thus, there is sufficient information from tyrosine markers to suggest that one of the structures is in a pseudo  $\beta$ -sheet arrangement consisting of tripeptide stacked units joined by hydrogen bonding and the other one is similar but with a more distorted long-range configuration. The results are important for the general field of peptide self-assembly as they further

confirm that even in simple model systems multiple supramolecular polymorphs, with consequently varying properties, may coexist in a single sample. Additional questions remain regarding the relative stability of each form, and the dynamic exchange between the soluble form and the more stable,  $\beta$ -sheet rich conformation.

## ACKNOWLEDGEMENTS

This research was supported by the University of Strathclyde and by the U.S. Air Force Office of Scientific Research (grant FA9550-19-1-0111). Research data associated with this paper will become available through the following link <https://doi.org/10.15129/2be8d3aa-1133-45df-930a-f6002852ad00>

## CONFLICT OF INTEREST

The authors declare no conflict of interest.

## ORCID

Sian Sloan-Dennison  <https://orcid.org/0000-0003-2473-1425>

## REFERENCES

- [1] R. V. Ulijn, A. Lampel, *Isr. J. Chem.* **2020**, *60*, 1129.
- [2] S. Zhang, *Nat. Biotechnol.* **2003**, *21*, 1171.
- [3] J. B. Matson, S. I. Stupp, *Chem. Commun.* **2012**, *48*, 26.
- [4] K. Kulkarni, N. Habil, M. P. Del Borgo, M.-I. Aguilar, *Front. Chem.* **2019**, *7*, 70.
- [5] E. Gazit, *Chem. Soc. Rev.* **2007**, *36*, 1263.
- [6] O. Khakshoor, J. S. Nowick, *Curr. Opin. Chem. Biol.* **2008**, *12*, 722.
- [7] A. A. Adzhubei, M. J. E. Sternberg, A. A. Makarov, *J. Mol. Biol.* **2013**, *425*, 2100.
- [8] L. J. Smith, K. M. Fiebig, H. Schwalbe, C. M. Dobson, *Folding Des.* **1996**, *1*, R95.
- [9] S.-K. Zhang, J.-W. Song, F. Gong, S.-B. Li, H.-Y. Chang, H.-M. Xie, H.-W. Gao, Y.-X. Tan, S.-P. Ji, *Sci. Rep.* **2016**, *6*, 27394.
- [10] J. S. Nowick, *Acc. Chem. Res.* **2008**, *41*, 1319.
- [11] S. Bieler, C. Soto, *Curr. Drug Targets* **2004**, *5*, 553.
- [12] N. J. Greenfield, *Nat. Protoc.* **2006**, *1*, 2876.
- [13] L. C. Serpell, P. E. Fraser, M. Sunde, *Methods in Enzymology*, Vol. 309, Academic Press, USA **1999**, 526.
- [14] A. T. Petkova, G. Buntkowsky, F. Dyda, R. D. Leapman, W. M. Yau, R. Tycko, *J. Mol. Biol.* **2004**, *335*, 247.
- [15] S. A. Oladepo, K. Xiong, Z. Hong, S. A. Asher, J. Handen, I. K. Lednev, *Chem. Rev.* **2012**, *112*, 2604.
- [16] B. Lekprasert, V. Korolkov, A. Falamas, V. Chis, C. J. Roberts, S. J. B. Tendler, I. Notinger, *Biomacromolecules* **2012**, *13*, 2181.
- [17] A. Lampel, S. A. McPhee, H.-A. Park, G. G. Scott, S. Humagain, D. R. Hekstra, B. Yoo, P. W. J. M. Frederix, T.-D. Li, R. R. Abzalimov, S. G. Greenbaum, T. Tuttle, C. Hu, C. J. Bettinger, R. V. Ulijn, *Science* **2017**, *356*, 1064.
- [18] S. M. M. Reddy, E. Raßlenberg, S. Sloan-Dennison, T. Hesketh, O. Silberbush, T. Tuttle, E. Smith, D. Graham, K. Faulds, R. V. Ulijn, N. Ashkenasy, A. Lampel, *Adv. Mater.* **2020**, *32*, 2003511.
- [19] B. Hernández, Y.-M. Coic, F. Pflüger, S. G. Kruglik, M. Ghomi, *J. Raman Spectrosc.* **2016**, *47*, 210.
- [20] A. E. Aliaga, I. Osorio-Roman, C. Garrido, P. Leyton, J. Cárcamo, E. Clavijo, J. S. Gómez-Jeria, G. Díaz F., M. M. Campos-Vallette, *Vib. Spectrosc.* **2009**, *50*, 131.
- [21] T. Weymuth, M. Reiher, *The Journal of Physical Chemistry B* **2013**, *117*, 11943.
- [22] B. Hernández, F. Pflüger, S. G. Kruglik, M. Ghomi, *J. Mol. Graphics Modell.* **2021**, *102*, 107790.
- [23] A. A. Profit, V. Felsen, J. Chinwong, E.-R. E. Mojica, R. Z. B. Desamero, *Proteins* **2013**, *81*, 690.
- [24] I. H. McColl, E. W. Blanch, A. C. Gill, A. G. O. Rhie, M. A. Ritchie, L. Hecht, K. Nielsen, L. D. Barron, *J. Am. Chem. Soc.* **2003**, *125*, 10019.
- [25] S. A. Overman, G. J. Thomas, *Biochemistry* **1999**, *38*, 4018.

## SUPPORTING INFORMATION

Additional supporting information may be found online in the Supporting Information section at the end of this article.

**How to cite this article:** Sloan-Dennison S, Lampel A, Raßlenberg E, et al. Elucidation of the structure of supramolecular polymorphs in peptide nanofibres using Raman spectroscopy. *J Raman Spectrosc.* 2021;1–7. <https://doi.org/10.1002/jrs.6121>